7-19-2017

Radiative Heat Transfer Analysis of Railroad Bearings for Wayside Hot-Box Detector Optimization

Arthur Mealer

Constantine Tarawneh

Stephen Crown

Proceedings of the 2017 Joint Rail Conference
JRC2017
April 4-7, 2017, Philadelphia, PA, USA

JRC2017-2260

RADIATIVE HEAT TRANSFER ANALYSIS OF RAILROAD BEARINGS FOR WAYSIDE HOT-BOX DETECTOR OPTIMIZATION

Arthur Mealer
Mechanical Engineering Department
University of Texas Rio Grande Valley
Edinburg, Texas 78539
arthur.mealer01@utrgv.edu

Dr. Constantine Tarawneh
Mechanical Engineering Department
University of Texas Rio Grande Valley
Edinburg, Texas 78539
constantine.tarawneh@utrgv.edu

Dr. Stephen Crown
Mechanical Engineering Department
University of Texas Rio Grande Valley
Edinburg, Texas 78539
stephen.crown@utrgv.edu

ABSTRACT

The railroad industry utilizes wayside detection systems to monitor the temperature of freight railcar bearings in service. The wayside hot-box detector (HBD) is a device that sits on the side of the tracks and uses a non-contact infrared sensor to determine the temperature of the train bearings as they roll over the detector. Various factors can affect the temperature measurements of these wayside detection systems. The class of the railroad bearing and its position on the axle relative to the position of the wayside detector can affect the temperature measurement. That is, the location on the bearing cup where the wayside infrared sensor reads the temperature varies depending on the bearing class (e.g., class K, F, G, E). Furthermore, environmental factors can also affect these temperature readings. The abovementioned factors can lead to measured temperatures that are significantly different than the actual operating temperatures of the bearings. In some cases, temperature readings collected by wayside detection systems did not indicate potential problems with some bearings, which led to costly derailments. Attempts by certain railroads to optimize the use of the temperature data acquired by these wayside detection systems has led to removal of bearings that were not problematic (about 40% of bearings removed were non-verified), resulting in costly delays and inefficiencies. To this end, the study presented here aims to investigate the efficacy of the wayside detection systems in measuring the railroad bearing operating temperature in order to optimize the use of these detection systems. A specialized single bearing dynamic test rig with a configuration that closely simulates the operating conditions of railroad bearings in service was designed and built by the University Transportation Center for Railway Safety (UTCRS) research team at the University of Texas Rio Grande Valley (UTRGV) for the purpose of this study. The test rig is equipped with a system that closely mimics the wayside detection system functionality and compares the infrared sensor temperature reading to contact thermocouple and bayonet temperature sensors fixed to the outside surface of the bearing cup. This direct comparison of the temperature data will provide a better understanding of the correlation between these temperatures under various loading levels, operating speeds, and bearing conditions (i.e. healthy versus defective), which will allow for an optimization of the wayside detectors. The impact on railway safety will be realized through optimized usage of current wayside detection systems and fewer nonverified bearings removed from service, which translates into fewer costly train stoppages and delays.

INTRODUCTION

Wayside hot-box detection (HBD) systems have been used extensively throughout the rail industry since the 1960's as a bearing health monitoring system. These detectors sit on the side of the tracks spaced about every 15 to 25 miles [1]. They have an infrared sensor that points upwards towards the railcar bearings, which senses the temperature difference between the bearing and a reference temperature as the train rolls by them [1]. Bearings that are flagged will trigger a warning indication to the train crews that the bearing needs to be removed to prevent a derailment [1], since bearings are capable of seizing and burning off between hot-box detector sites [2, 3].

Prior to 2002, the railroad industry experienced roughly 50 bearing failures every year that resulted in catastrophic derailments despite the use of wayside detectors [4]. After 2002, railways adopted the relative temperature performance system in order to improve the industries identification of problematic bearings [1]. Rather than looking at the absolute temperatures of particular bearings, this process involved the use of a K-value that would attempt to identify problematic bearings as a statistical outlier from a population of bearings

on one side of the train. Almost like a standard deviation, bearings whose K-values are significantly in excess of the average value on one side of the train are identified as bad bearings and then removed from service [1]. The problem with this system is that it has led to rail companies removing bearings that, upon disassembly and careful inspection, were found to be defect-free. A report prepared by Amsted Rail found that from 2001 to 2007, 40% of bearings removed from field service were non-verified [5]. This figure ranged from 24% to 60% during 2003 and 2004 [5]. These non-verified bearing removals translate into costly train delays and stoppages, maintenance times, and parts and supplies. Another problem stems from the fact that an extensive laboratory study performed on a large population of bearings has shown that not only is there no significant correlation with rises in temperature and size of defects on raceways, but that occasionally bearings with raceway defects can actually run at lower temperatures than the average operating temperatures of healthy (defect-free) bearings [5]. Furthermore, not all wayside detectors function in the same manner. There have been issues with some detectors alerting the train crew to the presence of a defect which turned out to be a false alarm, or it took the crew a very long time to locate the bearing in question; both instances resulting in costly train stoppages and delays.

There are various factors that can affect the readings taken by these wayside detectors. One factor is bearing size. Different classes (e.g., K, F, G, E) have different lengths and, therefore, the sensor points at a different location on the bearing cup (outer ring). Environmental factors can also affect the way these readings are taken. Inaccuracies in temperature readings have led to defective bearings not being detected, and in some extreme cases, to catastrophic derailments [2].

The Transportation Technology Center, Inc. (TTCI) performed testing on various HBD configurations from different vendors. The purpose of the study was to determine the most effective method in which to employ the HBDs so that the most accurate temperature measurement can be achieved. Temperature data analyzed in this study show the inaccuracies evident in the HBD infrared readings when compared to the corresponding thermocouple data [6]. Furthermore, the results of the study conclude that the error increases with increasing temperatures and it also depends on the location on the bearing where the readings are taken [6]. The abovementioned testing was performed at the TTCI Railroad Test Track. While effective, testing of this nature is very costly in terms of time, effort, and resources.

With this in mind, a single bearing dynamic test rig was designed and built by the UTCRS research team at UTRGV. This test rig closely simulates the conditions experienced by railcar bearings in field service. Since the bearing cannot travel in a laboratory setting, a carefully designed pneumatic system was put together to allow a non-contact infrared sensor to travel underneath the bearing in order to mimic the functionality of a HBD in field service. The experimental setup and techniques developed in this project facilitate the testing and optimization of HBD technologies in a laboratory setting, rather than in the field, which is a much more cost-effective and efficient method of testing. In order to reduce experimental iterations, the authors of this paper used a vertical positioning of the infrared sensor, which the TTCI study showed to be the most efficient [6].

EXPERIMENTAL PROCEDURE AND ANALYSIS

The single bearing tester (SBT) design, pictured in Figure 1, allows for the test bearing to be suspended at the end of an axle with an overhead load pressing down on the bearing through an adapter. This setup also allows for lateral and impact loads to be applied as needed to mimic the conditions a railroad bearing experiences in field service. In order to duplicate the manner in which a hot-box detector (HBD) senses the bearing's temperature in a laboratory setting, a method had to be devised to move the sensor underneath the bearing at a prescribed travel speed. Figure 2 shows how a pneumatic system was employed to accomplish this task. A near frictionless rail-cart system was designed and assembled that could transport the infrared temperature sensor under the bearing. Two IR break sensors, spaced strategically under the bearing area, were utilized to collect time measurements used to calculate the speed of the cart as it passed under the bearing. The cart was attached to a pneumatic cylinder fed by a four-way valve which employed an Arduino Uno as the controller.

Figure 1. Single Bearing Tester (SBT)

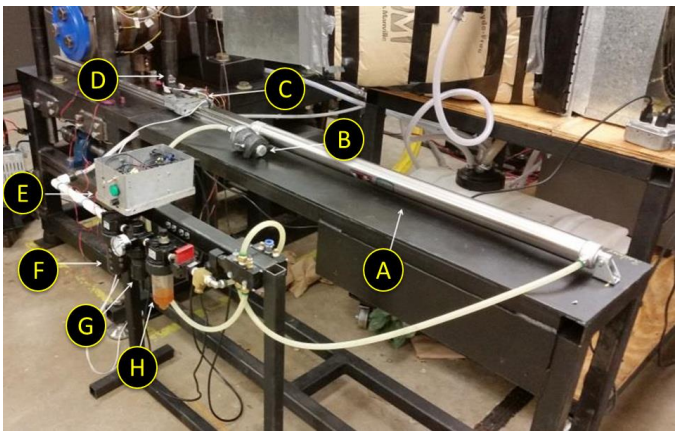

Figure 2. Hot-Box Detector (HBD) Simulation System, where [A] is the pneumatic cylinder, [B] is the quick exhaust valve, [C] is the cart, [D] is the infrared temperature sensor affixed to the cart, [E] is the control box, [F] is the pneumatic system filter followed by [G] the regulator and [H] the lubricator.

Figure 3 shows the HBD simulation system in action as the cart carrying the IR temperature sensor is traversing underneath the railroad bearing. The cart has a fixture that holds the sensor in place and can also be rotated. Four regions of interest were studied; outboard raceway, spacer ring region, inboard raceway, and the inboard seal region. Figure 4 shows those regions of interest marked on the cart that carries the IR sensor, while Figure 5 shows the paths under the bearing. Figure 6 shows those same regions of interest on the railroad bearing itself.

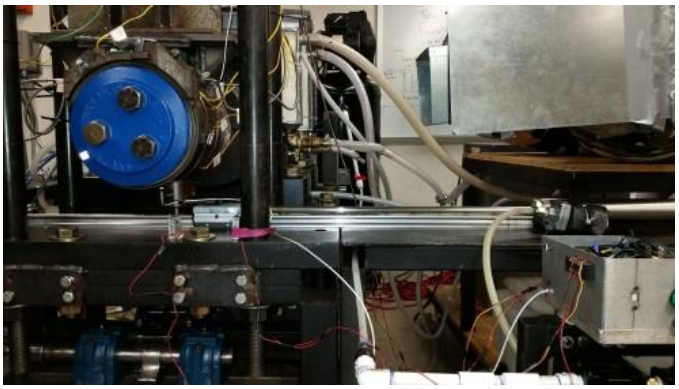

Figure 3. A picture of the devised hot-box detector simulation system as it transports the IR temperature sensor underneath the railroad test bearing.

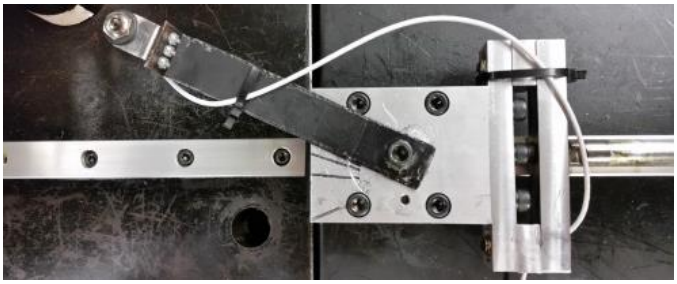

Figure 4. Top view of the cart that transports the IR sensor showing the markings on the cart that correspond to the four regions of interest. The bottom mark corresponds to the outboard raceway region followed by the spacer region markup, then the inboard raceway region markup. The current position of the IR sensor, shown in this picture, corresponds to the inboard seal region.

Figure 5. Picture showing the four paths that the IR sensor travels under the bearing. From right to left, the positions are the outboard raceway, the spacer region, the inboard raceway, and the inboard seal.

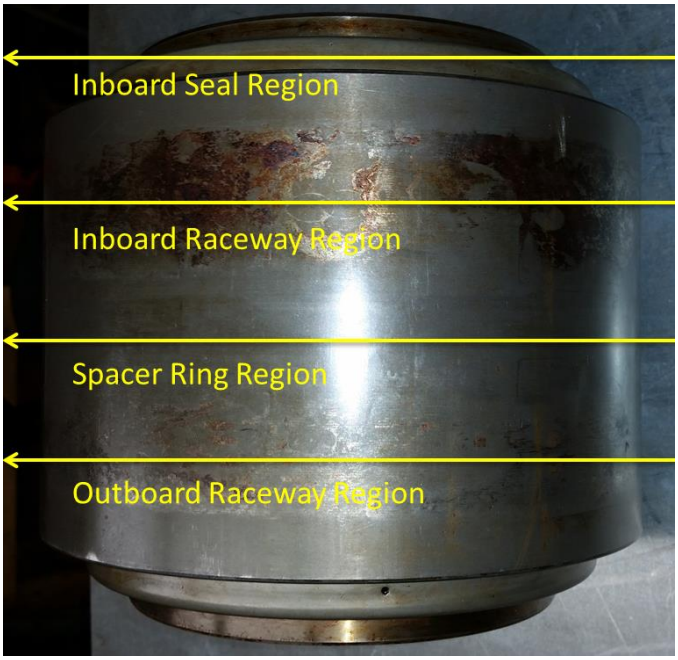

Figure 6. Picture showing the regions of interest that were scanned by the IR temperature sensor as it traversed under the railroad bearing.

The IR temperature sensor employed in the hot-box detector simulator system is a MICRO-EPSILON CTF-SF15-C3 miniature pyrometer. It has an optical resolution of 15:1, a temperature range of -50ºC to 975ºC and a spectral range of 8 to 14 micrometers. Its accuracy is within less than 1% with a resolution of less than 0.2ºC. Its response time is 4 milliseconds. Data was collected using the software CompactConnect which comes with the IR sensor from MICRO-EPSILON.

K-type thermocouple and bayonet thermocouple temperature data was collected through LabVIEW in twenty second intervals. Figure 7 depicts the locations of the thermocouples and bayonet thermocouples on the railroad bearing. All the thermocouples were attached to the bearing using a large hose clamp tightened along the spacer region of the bearing, as pictured in Figure 5. There were a total of seven thermocouples spaced around the circumference of the bearing, as indicated by the red dots in Figure 7. Four bayonets were also utilized, two at each of the two locations indicated by the black dots in Figure 7. The bayonet thermocouples monitored the cup temperature along the centers of the inboard and outboard raceways.

In order to examine cases with healthy and defective bearings, two bearings were utilized for this study. One bearing had a sizeable spall on one of the cup raceways that had developed naturally in previous experiments performed at the UTCRS, hereafter, called the “spalled” bearing. The second bearing used was a healthy (defect-free) bearing, hereafter, called the “control” bearing.

The parameters that were varied for this study included train traveling speed, bearing applied load, and IR sensor traveling velocity. Train traveling speed corresponds to the rotational speed at which the single bearing tester (SBT) motor turns the railroad bearing. The SBT is capable of testing train traveling speeds that range from 5 to 85 mph (8 to 137 km/h),

which correspond to bearing rotational speeds of 47 to 795 rpm. Speeds utilized in this study were 30, 45, 66, and 85 mph (48, 72, 106, and 137 km/h, respectively), which correspond to rotational speeds of 281, 421, 617, and 795 rpm, respectively. As can be seen in Figure 1, an overhead load is applied to the railroad bearing via a hydraulic cylinder. The two loads generally tested are 17% and 100% of a fully-loaded railcar. The 17% load setting corresponds to an empty (unloaded) railcar and translates to approximately 5848 lb_f (26 kN) per class K or F bearing, whereas, the 100% load setting corresponds to a fully-loaded railcar and translates to 34.4 kips (153 kN) per class K or F bearing. The data collected for this study utilized the 100% load setting since fully-loaded railcars are at a higher risk of bearing burn-off than empty railcars. The last parameter, IR sensor travel speed, is the descriptor of the speed at which the pneumatic cylinder pushes the sensor. It was desired to reach speeds of 30 mph (48 km/h), however, with the current setup, only speeds of up to 7 mph (11 km/h) were achieved. Higher IR sensor travel speeds can be achieved through some modifications to the current pneumatic system, but the goals of this study were met with the current system.

The Arduino Uno was employed to control the four-way valve of the HBD pneumatic simulation system using a timed program. To ensure that a new thermocouple data point was acquired for every run, the pneumatic system was engaged once every 30 seconds, shooting the IR temperature sensor under the railroad bearing at about 7 mph (11 km/h). The IR break sensors would send a signal to the Arduino reporting the time values to the computer. The IR sensor attached to the transporting cart reported the collected temperature data back to the CompactConnect software running on the same computer. Each trial would take about a minute, and each experiment would test all four positions previously mentioned (see Figure 5).

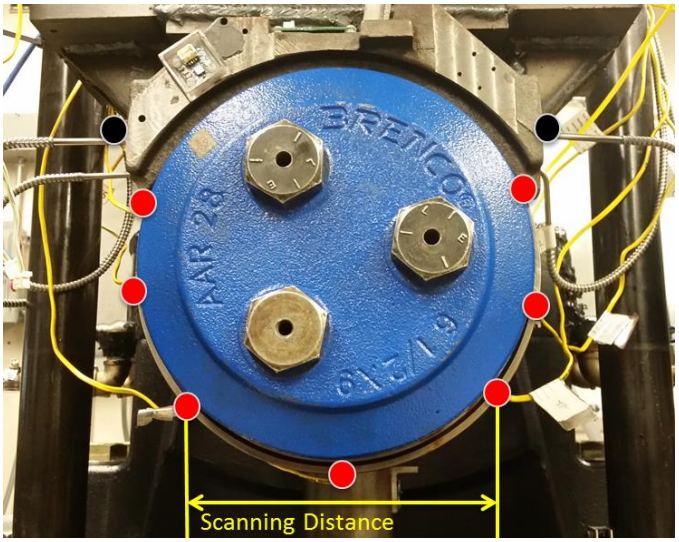

Figure 7. Thermocouple and bayonet thermocouple locations. Bayonet thermocouple locations indicated by the black dots, whereas, the regular thermocouple locations are indicated by the red dots. The IR temperature sensor scanning region is also shown on the figure.

MATLAB™ was employed to analyze all of the acquired temperature data. A script was written to gather all of the thermocouple data acquired by LabVIEW™, the time data collected by the Arduino, and the infrared temperature data obtained through the CompactConnect software. The complete data set was then processed by averaging the data points collected under the railroad bearing over the region labeled "scanning distance" in Figure 7. Then, the thermocouple data points that correspond to the times where the IR temperature sensor passed under the scanning distance were processed as well. Finally, the developed MATLAB™ script took all of the processed data and generated the plots that are shown in the following section.

Additional testing was conducted in order to establish a baseline for the bearing cup (outer ring) emissivity. The UTCRS possesses a large population of bearings with various stages of cup surface degradation. Twenty-five of those bearings were utilized for this additional testing. In order to minimize outside thermal influences, this testing was performed in an environmental chamber. Using a FLIR infrared camera, thermal images were taken that were later converted to temperature files. A thermocouple was used to measure the actual temperature of the bearing. A comparison was then carried out to generate an emissivity map of each bearing. Population statistics were then performed on the acquired data. Figure 8 shows a schematic diagram of the environmental chamber test setup.

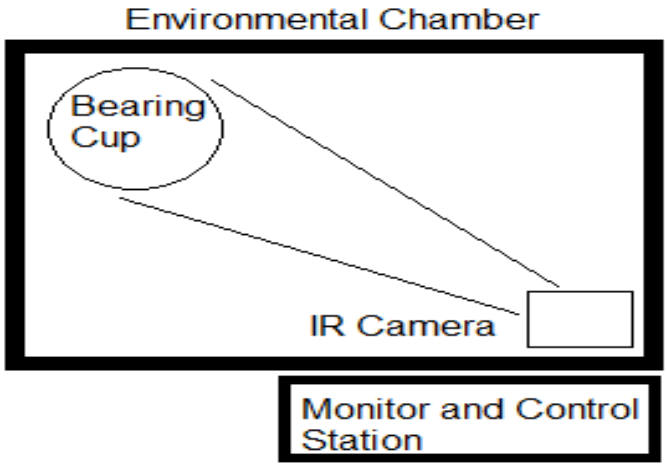

Figure 8. Schematic diagram of the test setup used for the bearing emissivity study. The thermal camera and the bearing were set up in an environmental chamber to limit any external thermal interference, and were controlled via a computer outside the chamber.

Testing was also conducted to establish the behavior, in a non-dynamic environment, of the MICRO-EPSILON infrared temperature sensor that was employed in the HBD simulation system. A bearing cup was placed in an oven with a K-type thermocouple attached as the control measurement. An infrared gun and the MICRO-EPSILON IR temperature sensor were then used to measure the temperature of the bearing at a number of different heat settings. Figure 9 is a picture of the setup used for this testing. The data of the IR temperature sensor agreed very well with those of the infrared gun and differed by no more than 2ºC (~4ºF) from the K-type thermocouple data at the highest heat setting tested (~100ºC).

Figure 9. Oven test setup. The K-type thermocouple can be seen attached using a hose clamp. The thermocouple multi-meter can be seen attached at the other end of the thermocouple.

RESULTS

In service, railroad bearings are loaded over the top hemisphere of the cup (outer ring) and unloaded over the bottom hemisphere of the cup. Hence, the temperature of the bearing tends to be higher at the top region where the load is applied, and decreases moving away from the top towards the bottom hemisphere of the cup. Figure 10 demonstrates this dynamic thermal performance for one of the bearings tested in this study. This plot shows temperature data from the seven thermocouples that are placed around the circumference of the bearing as well as the four bayonet thermocouples described in the experimental setup section and pictured in Figure 7. Looking at Figure 10, it becomes apparent that there is a distinct difference in the thermocouple temperatures based on their position around the bearing as mentioned earlier

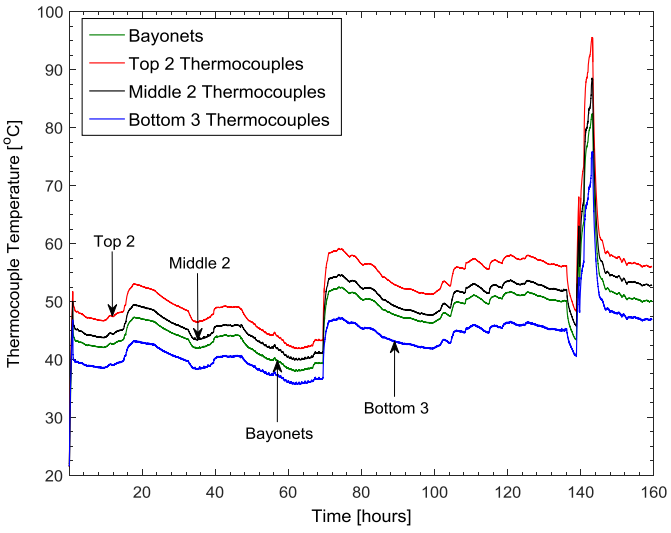

Figure 10. Thermocouple temperature histories for the duration of one experiment. The data shown represents the average temperature data of the thermocouples in each of the specified locations.

For the purpose of this study, it was decided to use the average temperature of the top two thermocouples as the most suitable predictor of the true bearing temperature since the top region of the bearing experiences the maximum applied load and the least thermal resistance. Hence, all other average temperature readings were compared against the average temperature of the top two thermocouples.

Figure 11 is a plot of the thermocouple readings versus the infrared sensor readings, which is very similar to the way the data was presented in the TTCI hot-box detector study [6]. For this plot, the ambient temperature associated with each reading, both thermocouple and infrared, was subtracted from the data points. The thermocouple data used in this plot was the average temperature of the top two thermocouples on the bearing. The results shown in Figure 11 exhibit very similar trends to what was concluded by the TTCI study [6]. One can observe that as the temperatures begin to rise, the infrared data begin to diverge further from the thermocouple readings.

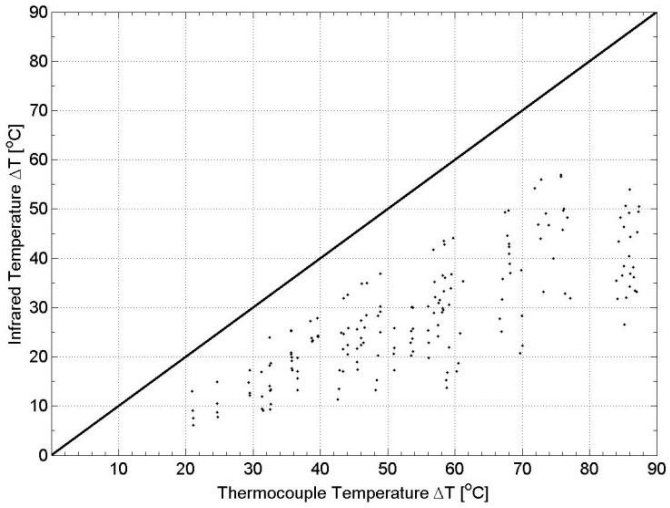

Figure 11. Infrared sensor temperature versus the average temperature of the top two thermocouples. The temperature data shown in this figure are temperature differences above the specific ambient temperature.

Figure 12 shows the thermocouple and infrared sensor temperatures versus train traveling speed. Note that the infrared sensor temperatures displayed in Figure 12 are average temperatures of all the data that was collected from the four sensor paths, shown in Figure 5, in much the same way a HBD infrared sensor in field service would scan a large portion of the bottom surface of the bearing. This data shows a clear discrepancy between the infrared sensor temperature data and the onboard thermocouple data (average temperature of top two thermocouples). This difference in temperature is hereafter called "IR sensor error." Figure 12 also shows that the IR sensor error increases as the train traveling speed increases. The bearing operating temperature increases with the train traveling speed since it is directly proportional to the bearing rotational speed. Since the bearing operating temperature is dependent upon its rotational speed, it would also seem that the IR sensor error (i.e., temperature difference between IR sensor readings and thermocouple readings) is also a function of temperature. The higher the bearing operating temperature is, the larger the IR sensor error, which is consistent with the results plotted in Figure 11. More importantly, it seems like the infrared sensor fails to

differentiate between a healthy defect-free bearing (i.e., control) and a defective bearing with a cup (outer ring) spall.

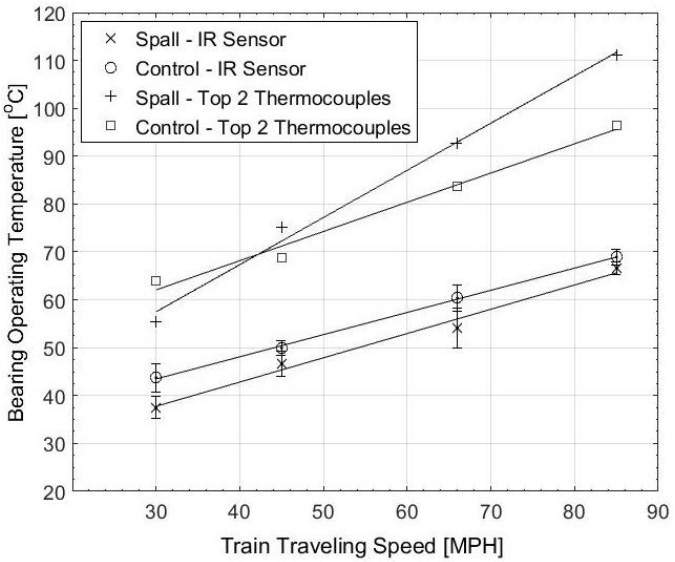

Figure 12. Infrared sensor and thermocouple average temperature readings versus the train traveling velocity.

The IR sensor error dependence on the bearing operating temperature is explored further in Figure 13, Figure 14, Figure 15, and Figure 16 which provide data for the outboard raceway, spacer ring, inboard raceway, and inboard seal regions, respectively. These figures examine the difference in temperature between the IR sensor reading and the top two thermocouple average temperatures for both the spalled and control bearings for all the regions tested (see Figure 5 and Figure 6). Figure 17 provides the average IR sensor error as a function of temperature for both the spalled and control test bearings for all the scanned regions.

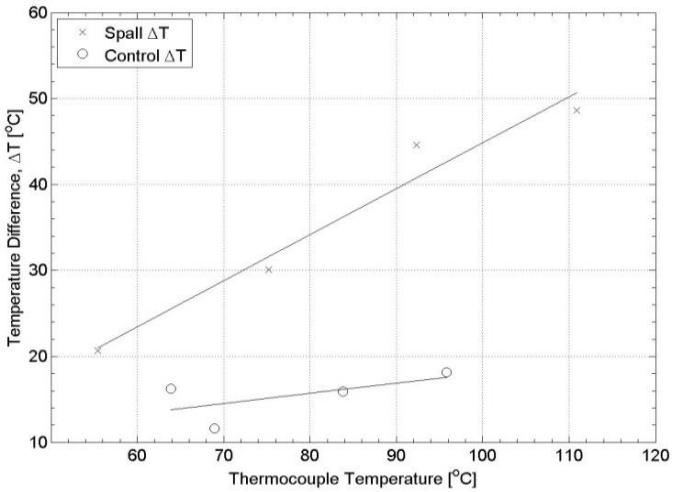

Figure 13. IR sensor error versus the top two thermocouple average temperature for both the spalled and control test bearings for the outboard raceway region.

Looking at Figure 13 through Figure 17, it can be seen that the IR sensor error increases almost linearly with the operating bearing temperature. It can also be observed that the increase in the IR sensor error is more drastic for the case of the defective (spalled) bearing as compared to the healthy (control) bearing, especially for the scanned outboard raceway region data. A definitive change in slope can be noticed in the cases for the outboard raceway, spacer ring, and inboard raceway regions, with the slope discrepancy getting less pronounced as we move inward from the outboard raceway region towards the inboard raceway region. Furthermore, it seems like the IR sensor error for the two test bearings, spalled and control, also gets closer as we move inward. For the case of the scanned inboard seal region data, Figure 16, it seems like the two slopes for the two test bearings are very similar with the IR sensor error being slightly higher for the control bearing as compared to the spalled bearing. One explanation for the latter behavior is that the inboard seal region does not seem to be sensitive to the effects of the spall present on the bearing cup (outer ring); hence, scanning the temperature of that region will not meaningfully differentiate between a healthy versus a defective bearing.

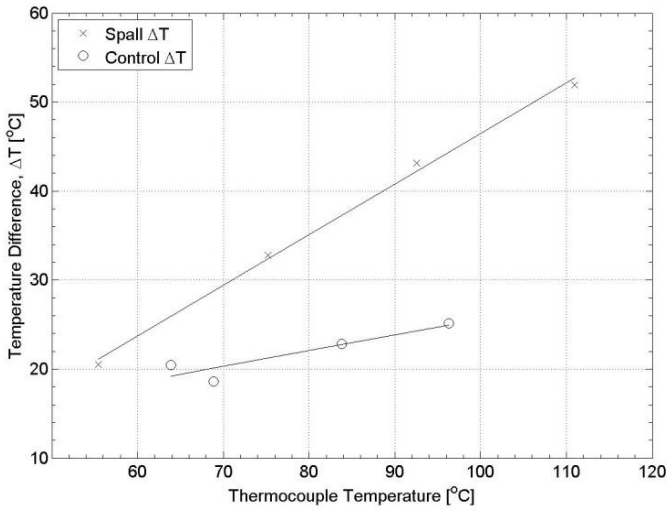

Figure 14. IR sensor error versus the top two thermocouple average temperature for both the spalled and control test bearings for the spacer ring region.

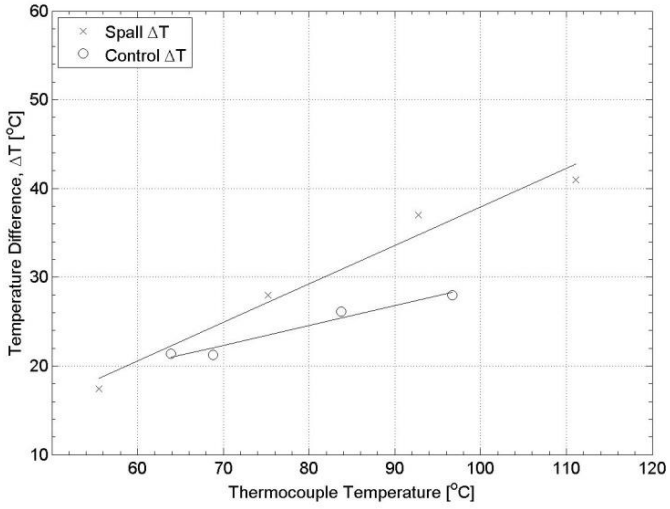

Figure 15. IR sensor error versus the top two thermocouple average temperature for both the spalled and control test bearings for the inboard raceway region.

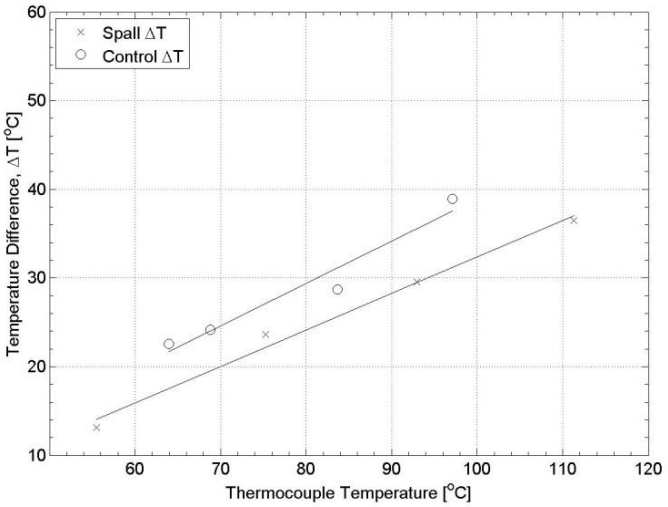

Figure 16. IR sensor error versus the top two thermocouple average temperature for both the spalled and control test bearings for the inboard seal region.

When looking at the average IR sensor error for all the scanned regions (Figure 17), the slope discrepancy is evident, with the spalled bearing having a larger IR sensor error than that of the control bearing for all bearing operating temperatures.

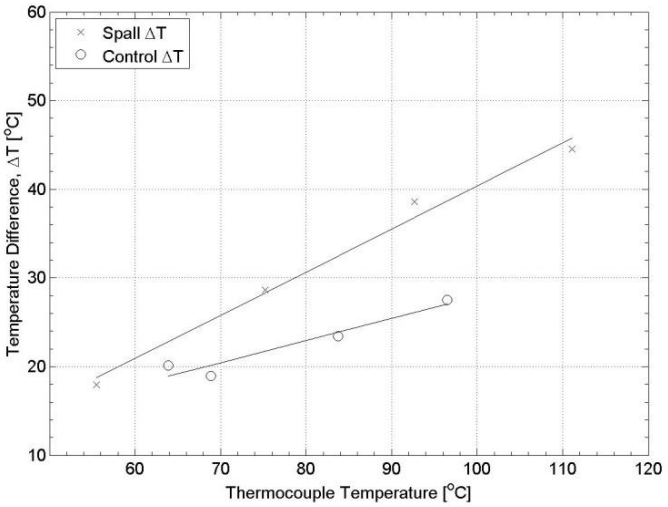

Figure 17. Average IR sensor error versus the top two thermocouple average temperature for both the spalled and control test bearings for all scanned regions.

Table 1 summarizes the results from the performed emissivity study. The data shows that a population of twenty-five bearings with various stages of cup surface degradation has very little variation in the emissivity of the cup outer surface. With a maximum emissivity of 0.96, a minimum of 0.86, and an overall average of 0.92, the temperature variations associated with this tight range are small enough to be neglected. The mean emissivity value of 0.92 was selected for the purposes of this study.

Table 2 provides the results from the infrared sensor oven test. The data indicates that there seems to be a consistent 7 to 9ºC difference between the MICRO-EPSILON IR sensor and the thermocouple readings used as the control measurement.

Table 1. Emissivity Study Results

Emissivity Population Statistics (25 Different Railroad Bearing Cups)	
Minimum Emissivity	0.86
Maximum Emissivity	0.96
Median Emissivity	0.92
Standard Deviation	0.02

Table 2: Infrared Sensor Oven Test Results [°C]

Set Point	IR Sensor	IR Gun	Thermocouple
60	51	54	58
80	70	73	78
100	90	89	98
120	109	112	118

CONCLUSIONS

Under normal bearing operating conditions, the top hemisphere of the railroad bearing is warmer than the bottom hemisphere, with the uppermost region of the bearing cup (outer ring), where the bearing adapter sits, being the warmest area. The latter behavior stems from the fact that the load is applied to the top of the bearing, leaving the bottom half of the bearing unloaded. Hence, it makes sense that the cup surface temperature decreases around the circumference of the bearing as we move away from the top towards the bottom. The results of this study indicate that this trend becomes even more pronounced with train traveling speed since the increase in rotational speed of the bearing is directly proportional to operating temperature of the bearing.

Relating the above findings to the data acquired from the IR temperature sensor employed in the hot-box detector (HBD) simulator system, there seems to be three main factors that contribute to the IR sensor error observed in Figure 13 through Figure 17. The constant error of 7 to 9°C shown in the oven test results (see Table 2) is one of those factors. The second factor is attributed to the increase in the temperature difference around the circumference of the bearing as a result of the increased rotational speed. However, the dynamic response of the IR temperature sensor is the third and most concerning factor. A thorough review of the collected data reveals that this error accounts for the largest percentage of the overall IR sensor error. The latter outcome holds true despite the fact that the selected IR temperature sensor employed in the HBD simulator system has a very good dynamic response time (~4 milliseconds), and simulates a train passing over a HBD with a velocity of only 7 mph (11 km/h). In field service, freight trains pass over HBDs at velocities far exceeding that of the UTCRS developed laboratory-based HBD simulator system, which contributes to greater IR sensor errors.

Moreover, as can be seen in Figure 13 through Figure 16, the IR sensor error is also dependent on the scanned region where the infrared temperature sensor is taking its reading. The field study performed by TTCI also concluded that the IR sensor error seemed to depend on the region of the bearing that was scanned by the wayside HBD [6]. Hence, the TTCI

field study findings support and validate the results obtained from this laboratory-based testing presented here.

In conclusion, the findings of this study indicate that it would be a very difficult task to attempt to accurately optimize the wayside HBD readings through programming. Considering the number of factors involved that will have to be accounted for, one would have to take the bearing operating temperature, bearing rotational speed, bearing loading condition, bearing class which dictates the lateral positioning of the bearing along the axle, as well as bearing health into consideration when attempting to estimate the IR sensor error. The complexity and interdependence of the aforementioned factors makes any attempt to simply adjust the hot-box detector programming very problematic to say the least. Nevertheless, if one wanted to simply obtain rough estimates of the IR sensor error in order to improve the readings of wayside HBDs, the results presented in Figure 12 and Figure 17 can be used for a wide range of train speeds and bearing operating temperatures for the cases of a healthy versus a defective (spalled) bearing. It should be kept in mind that this study tested only one defective bearing that has a spall on one of the cup (outer ring) raceways. The plan is to test bearings with other defects and see how that affects the IR sensor error.

Finally, the authors believe that the most accurate and reliable way to obtain the bearing operating temperature is through the use of onboard monitoring technologies that directly measure the bearing cup temperature at the loaded region of the bearing. Doing so eliminates the need to consider any of the complex factors discussed above.

ACKNOWLEDGEMENTS

This study was made possible by funding provided by the University Transportation Center for Railway Safety (UTCRS) through a USDOT Grant No. DTRT13-G-UTC59. The authors wish to thank Mr. Sam Olivarez for his tremendous help with instruction and assistance with the pneumatic systems. The authors also wish to thank Ms. Esmeralda Infante for her assistance on the bearing emissivity study she conducted during her participation in the HHMI High School research program.

REFERENCES

[1] Karunakaran, S., Snyder, T.W., 2007, "Bearing temperature performance in freight cars," *Proceedings Bearing Research Symposium*, sponsored by the AAR Research Program in conjunction with the ASME RTD Fall Conference, Chicago, IL, September 11-12.

[2] Transportation Safety Board of Canada, 2013, "Main Track Derailment," *Railway Investigation Report*, R13T0122.

[3] Barke, D., Chiu, W., 2005, "Structural Health Monitoring in the Railway Industry: A Review, Structural Health Monitoring 2005," 4(1): 81-93.

[4] Sneed, W.H., Smith, R.L., 1998, "On-Board Real-Time Railroad Bearing Defect Detection and Monitoring," *Proceedings of the 1998 ASME/IEEE Joint Rail Conference*, Philadelphia, PA, April 15-16.

[5] Tarawneh, C. M., Sotelo, L., 2016, "Temperature Profiles of Railroad Tapered Roller Bearings with Defective Inner and Outer Rings," *Proceedings of the 2016 ASME Joint Rail Conference*, Columbia, SC, April 12-15.

[6] Cline, J., Bonetto, A., & Sultana, T., 2014, "Evaluation of Hot Bearing Detector Technology Used to Identify Bearing Temperatures," *Technology Digest*, TD-14-017.